Influence of Chain Architecture on the Thermodynamic Properties of Lattice Polymer Solutions

Afshin Falsafi and William G. Madden*

Department of Chemical Engineering and Department of Materials Science and Engineering, Wayne State University, 5050 Anthony Wayne Drive, Detroit, Michigan 48202

Received December 28, 1992; Revised Manuscript Received June 3, 1993

ABSTRACT: Monte Carlo computer simulations have been performed on a three-dimensional simple-cubic lattice for mixtures of linear and branched chains with monomeric solvent molecules. Mixtures with chains of length 10 and of length 40 have been considered for both linear and branched architectures at a variety of polymer volume fractions. For the internal energy of mixing of athermal chains with solvent, the lattice cluster theory (LCT) is found to give predictions in reasonably good agreement with the results of the simulations, especially for short chains. At lower temperatures, the theory is not as satisfactory. However, it does prove to be more accurate for branched polymer with solvent than for linear polymer with solvent. The origins of the changes in the internal energy of mixing are understood in terms of additional internal contacts made possible by the presence of the branches. The effects of branching on the radii of gyration are also presented.

1. Introduction

Historically, lattice models have played a significant role in understanding the properties of polymer solutions, polymer melts, polymer blends, and polymer interfaces. First employed in the 1940s by Flory,[1-3] Huggins,[4,5] Miller,[6,7] and Guggenheim,[8-10] they are among the oldest models in polymer science. These theories were extended in the 1970s and 1980s to compressible systems by introducing empty sites into the formalism.[11-13] Cell models, close cousins to the lattice models in which the molecules are free to move within the confines of small periodically arranged boxes, were introduced for similar purposes.[14-16] The defects of all such models are readily apparent, and significant advances in the theory of condensed-phase polymer and polymer solutions using the methodologies of small-molecule liquids are now underway.[17-19] Still, lattice models remain the most tractable and best developed of all models for polymer solutions, polymer melts, and polymer blends. It is therefore reasonable to believe that a more complete understanding of lattice models for polymer systems can inform the search for improved approximations within the more realistic models. Recently, a new formulation of the partition function for lattice polymers has led to a tractable theory, the lattice cluster theory (LCT),[20-26] that can discriminate among different local architectures, a feature not yet available in *any* other theory, either on the lattice or in the continuum. A deeper understanding of how architecture affects the thermodynamics of polymer melts and solutions on the lattice can give insight into the extent to which such effects need be incorporated into promising new off-lattice theories. We present here the results of new computer simulations of lightly branched polymer on a three-dimensional cubic lattice and compare these with the predictions of lattice cluster theory.

The most famous result of any lattice theory for polymer solutions is the Flory–Huggins equation[1-4] for the Helmholtz free energy of mixing:

$$\frac{\Delta A^{\mathrm{MIX}}}{NkT} = \frac{\phi_s}{M_s}\ln(\phi_s) + \frac{\phi_p}{M_p}\ln(\phi_p) + \frac{z\Delta\epsilon}{2kT}\phi_s\phi_p \qquad (1)$$

where ϕ_s is the fraction of lattice sites occupied by solvent molecules and ϕ_p is the fraction of sites occupied by polymers. M_s is the "molecular weight" of solvent, the number of lattice sites occupied by one solvent molecule, and M_p is the "molecular weight" of polymer, the number of lattice sites occupied by one polymer molecule. The quantity $\Delta\epsilon$ is the interchange energy defined by

$$\Delta\epsilon = 2\epsilon_{ps} - \epsilon_{ss} - \epsilon_{pp} \qquad (2)$$

where ϵ_{ss}, ϵ_{pp}, and ϵ_{ps} are the interaction energies of nearest-neighbor beads of the indicated species and z is the coordination number of the lattice. The quantity $z\Delta\epsilon/k_BT$ is usually identified as the Flory χ parameter and is allowed to vary with temperature, pressure, composition, and chain length when the theory is applied to experimental data on real polymer systems. In a strict lattice interpretation of the Flory–Huggins equation, the right-hand side of eq 1 is linear in $\Delta\epsilon/k_BT$ and the theory is thus a first-order perturbation treatment of polymer solutions with fairly drastic approximations both for the athermal reference solution and for the energetic correction term. The deficiencies of the Flory–Huggins equation have been acknowledged since its inception but were not quantified for concentrated polymer solutions or compressible melts until direct comparisons were made with computer simulations by Dickman, Hall, and co-workers,[27-31] Madden, Freed, and co-workers,[32,33] and (for polymer blends) Sariban, Binder, and co-workers.[34-37]

Huggins,[4,5] Miller,[6,7] and Guggenheim[8-10] derived lattice theories for polymer solutions that, in an average fashion, keep a more careful track of the presence of covalently bonded sites on a typical polymer bead. All three workers produced equivalent theories for athermal polymer solutions, but each treated the energetics in a slightly different way. Guggenheim invoked his quasichemical approximation[9] to account for the solution energetics, and this approach seems to be the most sophisticated and self-consistent extension of the athermal results to finite temperatures. The quasichemical expression for the free energy of mixing is given by

$$\frac{\Delta A^{\mathrm{MIX}}}{NkT} = \frac{\phi_s}{M_s}\ln(\phi_s) + \frac{\phi_p}{M_p}\ln(\phi_p) + \frac{z}{2}\left[\frac{q_s\phi_s}{M_s}\ln\left(\frac{\theta_s}{\phi_s}\right) + \frac{q_p\phi_p}{M_p}\ln\left(\frac{\theta_p}{\phi_p}\right)\right] + \frac{z\Delta\epsilon}{2kT}\phi_s\theta_p\Gamma \qquad (3)$$

where

$$\Gamma = \frac{2}{1 + [(\theta_s - \theta_p)^2 - 4\theta_p\theta_s e^{\Delta\epsilon/kT}]^{1/2}} \qquad (4)$$

$\theta_i = q_iN_i/(q_sN_s + q_pN_p)$ is the surface fractions of species

0024-9297/94/2227-3094$04.50/0

i (=p or s), and $zq_i = M_i(z-2)+2$. In these studies, the solvent will be monomeric and hence $q_s = 1$.

More recently, Freed and co-workers[20-26,32,33] have devised a formally rigorous theory for the thermodynamics of molecular lattice solutions based on a clever recasting of the partition function and on a dual expansion of the free energy in $1/z$ and in $\Delta\epsilon/kT$ for a variety of molecular architectures on a simple d-dimensional hypercubic lattice. The resulting expressions are quite complicated but are of the form

$$\frac{\Delta A^{MIX}}{NkT} = a_0 + a_1\left(\frac{\Delta\epsilon}{kT}\right) + a_2\left(\frac{\Delta\epsilon}{kT}\right)^2 + a_3\left(\frac{\Delta\epsilon}{kT}\right)^3 + \dots \quad (5)$$

where the coefficients a_n are themselves expanded in z^{-1}

$$a_n = \zeta_n^{(0)} + \zeta_n^{(1)}\frac{1}{z} + \zeta_n^{(2)}\left(\frac{1}{z}\right)^2 + \dots \quad (6)$$

Each of the coefficients $\zeta_n^{(i)}$ is independent of temperature but depends on volume fraction, molecular weight, lattice architecture, and molecular connectivity. All coefficients can be evaluated analytically, but an increasingly large number of individual integrals (represented in the theory as Mayer-like graphs) must be evaluated to produce higher order terms in the expansions.

At present, closed-form expressions are available to second order in $\Delta\epsilon$ and to second order in $1/z$. Approximate corrections to zeroth order in $1/z$ are available for the third- and fourth-order term in $\Delta\epsilon$. These zeroth-order expressions provide higher order energy corrections in the spirit of the Flory–Huggins theory, and at this level, the theory is called the extended mean field theory (EMF). Like the Flory–Huggins theory, the extended mean field expressions do not take into account the inaccessibility of some neighboring sites necessarily occupied by covalently bonded neighbors from the same chain. It is essential to keep in mind the distinction between the lattice cluster theory as a powerful formalism and the several existing implementations. Calculations performed within the LCT carry eq 5 through the a_2 term and are designated LCT2. Both a_1 and a_2 are calculated from eq 6 including terms through z^{-2}. When the zeroth-order EMF expressions for a_3 and a_4 are added, we designate the results LCT2-2. Dudowicz et al. found that the EMF a_3 and a_4 were of negligible magnitude for linear chains and monomeric solvent, and we find that this also holds when the chains have branched architecture. Though the results presented here were all obtained with LCT2-2, the distinction between the results of LCT2 and LCT2-2 would be difficult to discern in the figures presented below.

When the expansions in the lattice cluster theory converge, that formalism is capable of producing an arbitrarily accurate result, including correlations arising from chain connectivity. In such circumstances, any errors observed are solely a consequence of truncation and can be corrected by extending the theory to higher order terms in $1/z$ and in $\Delta\epsilon$. The expansion in $\Delta\epsilon$ is well established in condensed matter theory and can be expected to converge rapidly at high temperatures and at high volume fraction of polymer but not near a critical singularity nor when the interactions are long ranged, as in ionomer systems.

The expansion in $1/z$ is more problematic. At moderate-to-high polymer volume fractions, the screening of chains by one another requires that only the local environment of a bead be well represented, and a truncated $1/z$ expansion seems adequate to this task. This is arguably why all of the theories work quite well at high volume fraction of polymer. At lower volume fractions and lower temperatures, the connectivity of the polymer becomes increasingly important and the changes in intramolecular conformations become increasingly significant. For linear chains with monomeric solvent, both the first- and second-order terms in $\Delta\epsilon$ have been examined independently.[32,33] In each case, a second-order expansion in $1/z$ is in excellent agreement with computer simulation results at all volume fractions. It is not known, however, whether this will remain true for higher order terms in $\Delta\epsilon$. In principle, we can expect these expansions to fail at very low ϕ_p, where they must reproduce the subtle thermodynamics of an ensemble of isolated chains and where connectivity constraints dominate. This regime is normally regarded as outside the bounds of the conventional lattice theories, but their predictions in this region nevertheless influence the coexistence curve on the dilute-polymer side. A completely satisfactory theory for dilute solutions based on the LCT will probably require a renormalization involving an approximate systematic summation of graphs to all orders. Efforts in this direction are now underway.

An alternative lattice theory based on the Born–Green–Yvon (BGY) hierarchy and the Kirkwood superposition approximation, devised by Lipson, Guillet, and Whittington[38] has recently been extended and improved by Lipson and co-workers.[39-41] This approach provides a somewhat different route to the energetic corrections for polymer solutions, employing independent results from some other theory for the athermal reference system. Versions based on both the athermal Flory–Huggins theory and the Huggins–Miller–Guggenheim (HMG) theory have recently been produced. The BGY lattice theory cannot transcend the intrinsic approximations used for the athermal system, but under some circumstances it may provide more realistic temperature dependences than appear in the traditional theories.

Available simulation studies[32,33] of polymer solutions show that the Flory–Huggins theory and the extended mean field version of the lattice cluster theory are not satisfactory except at very high volume fraction of polymer. The version of BGY lattice theory based on the Flory–Huggins reference system seems to share the same defects. LCT2, LCT2-2, the Guggenheim quasichemical theory (GQC), and the HMG/BGY combination all seem to produce significantly better results for the free energy of mixing. All give highly accurate first-order perturbation terms for the free energy of mixing and reasonably good second-order terms. The energetics of mixing for LCT2, for LCT2-2, and for the preferred implementation of the HMG/BGY theory are very similar and considerably better than that of GQC, the best of the traditional lattice theories. LCT2 has also been shown to give rather good coexistence curves for linear chains of length 100 in monomeric solvent. It has also been shown to predict the excess chemical potential of solvent (or "lattice pressure") in athermal solutions of polymer with monomeric solvent. However, all these theories give internal energies of mixing that are in poor agreement with computer simulation at intermediate volume fractions and moderately low temperatures ($kT/\Delta\epsilon \leq 3$). This indicates third- and higher-order terms in the LCT are substantial and are not properly incorporated at the EMF level. Dudowicz et al. attribute this to the increasing importance of the chain connectivity. Serious deficiencies in the energies of mixing and in coexistence curves have also been noted by Sariban and Binder for polymer blends and are probably of similar origin. In an attempt to circumvent the remaining errors in all the lattice theories, Lambert et al.[47] have recently fit new simulation data for the energies of mixing to suitable

functional forms. This procedure leads to a highly accurate representation of the simulation results of linear chains, but new data would have to be accumulated and fit for each additional architecture of interest.

Nearly all the criticisms of the LCT apply to the other lattice theories as well, since none of these has an adequate temperature dependence at intermediate volume fractions. In those theories, however, there is no overarching framework that suggests systematic improvements. (The BGY approach admits to improvements on the superposition approximation, but improvements in the properties of the reference system and the influence of connectivity can at present be addressed only by inclusion of the results of some independent theory for the reference athermal free energy of mixing.) Only the LCT includes the effects of chain architecture in the expression for the free energy. In an attempt to test the LCT in this regard and to further understand the physical predictions of the lattice model, we present here the results of computer simulations for the energetics of mixing of a monomeric solvent with a linear lattice polymer (a lattice cartoon of polyethylene) and with a branched lattice polymer ("lattice polypropylene").

2. Simulation Details

In order to examine both linear and branched chains, we have employed a modification of the traditional Verdier–Stockmayer algorithm[42] for simulation of chains on a simple-cubic lattice. Our version of the algorithm includes three distinct attempted moves:

(1) *Monovalent beads*: A bead at the end of chain or at the end of a branch may move to a randomly chosen site adjacent to its covalently bonded neighbor.

(2) *Divalent beads*: An interior bead that is not a branch point and which is in a bent configuration may move to a site on the opposite corner of a square defined by the bead in question and its two covalently bonded neighbors.

(3) *Higher valences*: An interior bead from which one or more branches emerge and which is in a bent configuration with respect to its two backbone neighbors is moved to the opposite corner of the square defined above for divalent beads. The branches are then grown from the new site as unbiased random walks of appropriate length beginning at the new position of the backbone bead.

Attempted moves are accepted according to the usual canonical criterion, $\exp(-\beta\Delta E) > \xi$, where ξ is a random number uniformly distributed in the interval (0,1).

This scheme differs from that of Verdier and Stockmayer in how the beads of higher valence are treated. All three processes move material on the lattice and are sensitive to volume fraction. The third process can become especially slow for highly branched molecules or for molecules with very long branches. At moderate and high volume fractions, the algorithm described above will not result in an adequate acceptance rate unless the total number of beads in the pendant side chains is kept small. In this work, we consider only side chains with at most a single bead. More complicated methods have been successfully employed in the past to enhance the efficiency of lattice algorithms for linear chains. Presumably, these methods could also be extended by adding a growth step for side chains when one or more of the moved beads is of higher valence. However, the presence of a large number of trivalent beads would complicate the coding and further reduce the already low acceptance rate for these more elaborate moves. It therefore seems sensible to keep the algorithm as simple as possible.

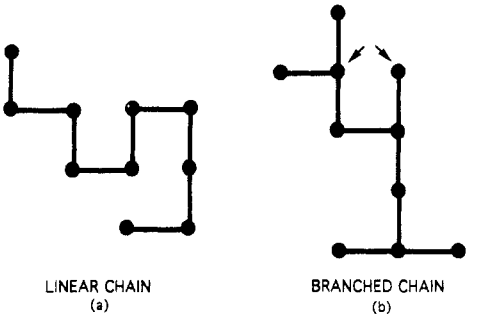

Figure 1. Polymer architectures considered in this study (M = 10). The arrows indicate a local configuration discussed in the text.

For the particular branched architecture considered in this communication, it is possible to devise a pseudoreactive algorithm along the lines of that employed by Mansfield,[43] by Olaj et al.,[44] and by Madden and coworkers[32,33,45] in their studies of lattice polymer thermodynamics for linear chains. Indeed, Mathur et al.[46] have used a version of this method to study the mobility of small side chains in the neighborhood of a wall for a vacancy-free lattice. These simulation methods can enhance the efficiency of the algorithm by several orders of magnitude but they necessarily produce a polydisperse sample. This is not in principle a deficiency in the method since real polymer samples are usually polydisperse. However, the polydispersity in chain length must be kept fairly narrow if meaningful comparison is to be made with a theory for a monodisperse sample. Since our attention here will be focused on the rather small differences in the internal energy of mixing of monomeric solvent with branched and linear polymers, we have opted for a more traditional simulation method to avoid any questions concerning the possible distortion of the results arising from polydispersity.

The simulations were performed on uniform bulk sample confined to a box of dimensions $L \times L \times L$ with periodic boundary conditions in all directions. For most of the calculations reported here, $L = 20$, but several simulations were performed for $L = 40$ to ensure that finite size effects are not significant for the calculated quantities. The results of these tests show that $L = 20$ is entirely adequate for chains of molecular weight 40 or less. To minimize the detrimental effects of branching on the movement of trivalent beads, we confine our studies to branched molecules with single-bead substituents placed at every other bead on the chain backbone. The linear and branched architectures of the chains simulated here are illustrated in Figure 1 for a molecular weight (M) of ten beads.

Initial configurations were typically generated by a modification of the growth algorithm described in ref 45. For volume fractions of 0.5 or less it was possible to lay down all the chains directly, without any intermediate bead movement. At higher volume fractions, an appropriate number of short chains are laid down to achieve an initial volume fraction of about 0.5. These short chains are allowed to move using the algorithm described above. Periodically, attempts are made to lengthen the chains or place branch beads along the chain until the appropriate number of chains of desired length and architecture are achieved. Configurational snapshots are taken for detailed analysis at suitable intervals, typically every 10 or 30 passes (attempted moves per bead). Running block averages are made over intervals of 10 000–30 000 passes. These short running blocks can then be combined in various ways into larger subblocks to assess the statistical uncertainties in

the results. The overall lengths of the runs vary from 300 000 to 3 000 000 moves per bead as dictated by ongoing statistical analysis of the block averages. As expected, the longest runs were required for branched systems at high molecular weight and high volume fraction.

The ensemble average of the number of polymer–polymer contacts $\langle N_{pp} \rangle$ and the energy of mixing ΔE^{MIX} were calculated from

$$\frac{\Delta E^{MIX}}{N} = \left(\frac{\langle N_{pp} \rangle}{N} - \frac{z}{2}\phi_p \right) \Delta\epsilon \qquad (7)$$

where N is the total number of lattice sites, ϕ_p is the volume fraction of polymer, and z is the coordination number of the lattice (here, $z = 6$). The details of our algorithm are such that the quantity $\langle N_{pp} \rangle$ includes nearest-neighbor beads that are covalently bonded. This feature merely shifts the zero of energy and is eliminated in the subtractions required to calculates ΔE^{MIX}. Except for the largest chains at the highest polymer volume fraction considered here ($\phi = 0.8$), we can detect no correlation of the energy of mixing to the initial configuration after about 30 000 passes. For safety's sake, 100 000 passes were discarded prior to taking equilibrium averages. The initial configurations for simulations at finite temperature were normally obtained from the final configuration of an athermal simulation for chains of the same volume fraction, molecular weight, and chain architecture. An additional equilibration step of at least 100 000 passes was included before equilibrium averages were taken. Partitions of the runs into 5–25 large subblocks gave consistent estimates for the standard deviation of the means. These statistical uncertainties for the energy of mixing are typically better than 1 part in 2000 and vary from 1 part in 500 to 1 part in 6000, depending on chain architecture, molecular weight, volume fraction, and duration of the run. This level of uncertainty allows for a more detailed comparison than would otherwise be warranted.

In addition to the energy of mixing, a variety of properties for global chain configuration were monitored, including the Cartesian components of the mean square of radius of gyration and the mean square end-to-end vector. (The branched chain has two equivalent "end beads" at each end of the chain. We arbitrarily designated one such bead at each end for calculation of the end-to-end vector.) There is indirect evidence that for a few of the shortest runs at $M = 40$, these global properties show some slight correlation to the initial configuration. It is not uncommon for certain properties, particularly global properties of the individual chains to relax more slowly than others. All available evidence shows that the internal energy of mixing is insensitive to minor configurational readjustments on such large length scales, and indeed there are no corresponding anomalies in the calculated internal energies of mixing.

3. Results and Discussion

Because of connectivity restrictions, the branched chains shown in Figure 1 must be of molecular weight $M = 3n + 1$, where n is an integer. We have performed extensive calculations (in excess of 100 independent runs) on linear and branched chains for $M = 10$ ($n = 3$) and for $M = 40$ ($n = 13$) at polymer volume fractions ranging from $\phi = 0.2$ to $\phi = 0.8$. The remaining sites may be regarded as occupied by either vacancies or monomeric solvent molecules depending on whether the system corresponds to a compressible pure polymer or an incompressible binary solution. Two reduced temperatures were considered: $T = \infty$ and $T = 3$ (in units of $\Delta\epsilon/k_B$). The first corresponds to an athermal system and the second to a temperature slightly above the critical temperature of the system. Figure 2 compares the energy of mixing per lattice site (in units of $\Delta\epsilon$) for chains of all lengths and architectures under athermal conditions. At the lowest volume fractions, the effects of molecular weight are more pronounced than those of architecture, and the energies of mixing for chains of length 40 are consequently lower than those for chains of length 10 regardless of chain architecture. The energy of mixing for linear chains is lower than that for branched chains of the same molecular weight at all volume fractions, but the differences are very small at the lowest volume fractions. At intermediate volume fractions, the effects of architecture become much more pronounced, and the energies of mixing for branched chains of length 40 are found to be larger than for linear chains of length 10. At the highest volume fractions, the energies of mixing coalesce into pairs based on architecture rather than chain length. The two branched systems have similar energies of mixing as do the two linear systems, with a higher energy of mixing in the branched case.

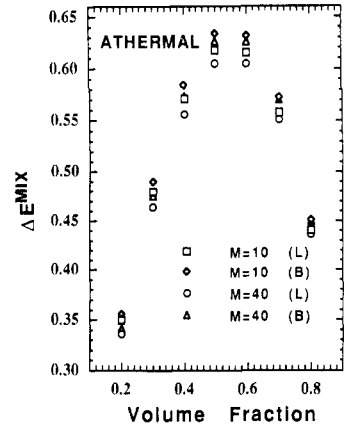

Figure 2. Monte Carlo energies of mixing $\Delta E^{MIX}/(N\Delta\epsilon)$ as a function of polymer volume fraction ϕ_p for athermal solutions ($T = \infty$) of polymer chains in single-bead solvents. (L) = linear; (B) = branched.

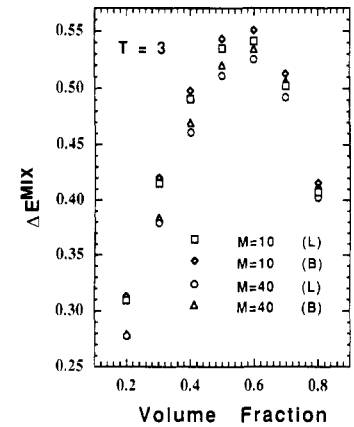

Figure 3. Monte Carlo energies of mixing $\Delta E^{MIX}/(N\Delta\epsilon)$ as a function of polymer volume fraction ϕ_p for solutions of polymer chains in single-bead solvents at a reduced temperature $T = 3$.

Figure 3 provides a similar comparison at $T = 3$. At low volume fractions, the effect of molecular weight is considerably larger, and the grouping of the results into two distinct sets persists at substantially higher volume fractions (up to $\phi = 0.6$). Conversely, there is a smaller effect of chain architecture at intermediate volume fractions than was observed in the athermal case, also contributing to the separation of the curves into two distinct groups. The reduction in the internal energies relative to the athermal values requires that the number

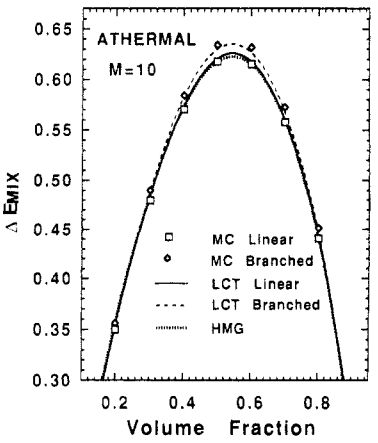

Figure 4. Comparison of Monte Carlo results and lattice theory predictions for the athermal ($T = \infty$) energy of mixing $\Delta E^{MIX}/(N\Delta\epsilon)$ of a single-bead solvent with polymer of length 10.

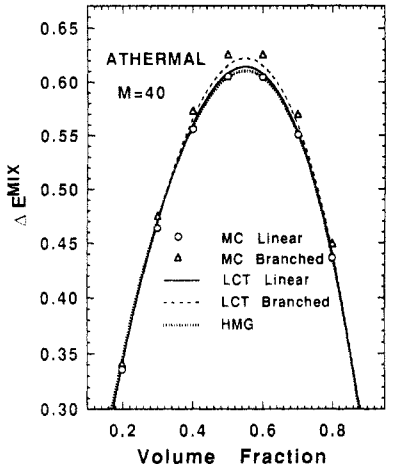

Figure 5. Comparison of Monte Carlo results and lattice theory predictions for the athermal ($T = \infty$) energy of mixing $\Delta E^{MIX}/(N\Delta\epsilon)$ of a single-bead solvent with polymer of length 40.

of solvent polymer contacts be reduced at the lower temperature. These observations may in part be associated with the expected compaction of the chains as solvent is excluded from the interior of the chain. At the highest volume fraction, no obvious trend is apparent, but the energies of mixing are all quite similar.

As noted earlier, only the lattice cluster theory makes any predictions concerning the effect of chain architecture on the thermodynamic properties of the solution. Figure 4 compares the predictions of LCT2-2 with simulation for linear and branched athermal chains of length $M = 10$. Also shown is the energy of mixing obtained from the athermal Huggins–Miller–Guggenheim theory, which is, by far, the best of the classic lattice theories and is the preferred reference result for the latest version of the BGY theory. Quite clearly, the LCT predicts the correct behavior of the chains as branching is introduced. Figure 5 makes a similar comparison for chains of length 40. Here, the simulation results show a larger effect of architecture at intermediate volume fractions than was observed at the lower molecular weight. The LCT, however, does not predict these larger differences, though it remains qualitatively correct. For branched chains at $\phi = 0.8$, we found it necessary to perform a run of 3×10^6 moves per bead to achieve adequate statistical uncertainty and independence from the starting configuration. In both the $M = 10$ and $M = 40$ simulations, it seems that the linear and branched LCT curves converge more rapidly at high volume fractions than the corresponding simulation data.

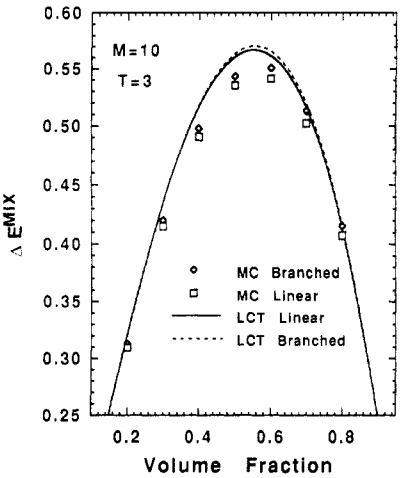

Figure 6. Comparison of Monte Carlo results and lattice theory predictions for the energy of mixing $\Delta E^{MIX}/(N\Delta\epsilon)$ of a single-bead solvent with polymer of length 10 at a reduced temperature $T = 3$.

Any comparison of athermal LCT and the HMG theory must be based on tiny differences in the energies of mixing. We believe that our results are sufficiently accurate that we may make a more detailed comparison than was possible in the earlier reports of Madden et al.[32] and Dudowicz et al.[33] At intermediate volume fractions ($0.4 < \phi < 0.7$), the HMG results for linear chains seem very slightly more accurate than those of LCT2-2. However, LCT2-2 becomes superior to the HMG theory for $\phi \leq 0.3$. This is not surprising since the connectivity of the chains is expected to become increasingly important at low volume fractions, where intrachain contacts begin to dominate the energetics. Only the LCT includes any connectivity correlations. Why the HMG theory should be particularly accurate for linear chains is somewhat of a mystery. Though the linear architecture of the chains was implicitly included in Guggenheim's derivation, no clear contributions of that architecture survive the subtractions that lead to the HMG expression for the free energy of mixing, and the HMG expressions can be rederived without any assumptions as to chain architecture. Possibly, the special accuracy of the HMG theory for linear chains arises from its treatment of all beads in an equivalent and averaged fashion. An approximation of that sort makes more sense when nearly all beads are divalent than when they are the heterogeneous mix of monovalent, divalent, and trivalent beads that characterizes the branched system under consideration here.

Figures 6 and 7 make similar comparisons for chains of length 10 and 40 at $T = 3$. Dudowicz et al.[33] established that LCT2 gives substantially better energies of mixing for chains of length 100 than do any of the traditional lattice theories. More recently, Lipson[39,40] has shown that a particular version of the Guggenheim-based BGY theory produces energies of mixing quite competitive with those of LCT2 and LCT2-2 for linear polymer and monomeric solvent. However, Dudowicz et al. also found that, at intermediate and low volume fractions, there are significant discrepancies between the predictions of LCT2 and the results of computer simulations. The BGY theory errs in about the same fashion. Similar failings are seen for the slightly shorter linear and branched chains examined here. To avoid confusing the graphs, no results from other lattice theories are shown. Except for HMG/BGY, the results of these theories are markedly poorer than those obtained from LCT2-2 for linear chains and, of course, are all silent concerning branched chains.

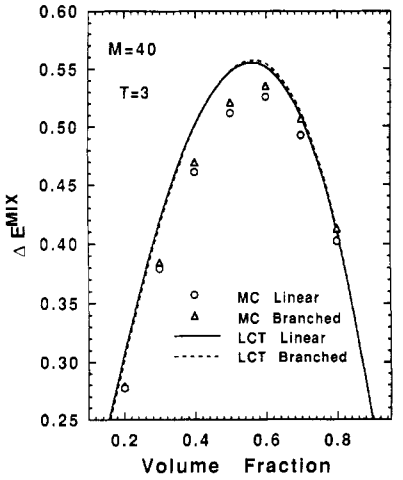

Figure 7. Comparison of Monte Carlo results and lattice theory predictions for the energy of mixing $\Delta E^{MIX}/(N\Delta\epsilon)$ of a single-bead solvent with polymer of length 40 at a reduced temperature $T = 3$.

The internal energies of mixing in Figures 6 and 7 for the linear and branched systems are seen to be smaller than the analogous athermal results. The LCT2-2 calculations give very similar energies of mixing for the two architectures at all volume fractions, a trend not consistent with the computer simulations. A close examination shows that LCT2-2 predicts that the branched system has energies of mixing slightly larger than those of the linear system at higher volume fractions and has slightly smaller energies of mixing at lower volume fractions. In the simulations, the branched system is always found to have the higher internal energy of mixing, though we cannot rule out a crossing at volume fractions lower than 0.2. At the outset of this work, we had hopes that the available implementations of the LCT could be used as the basis of a kind of perturbation calculation of the effects of structure on the thermodynamic properties of polymer solutions. The reference state of such a calculation would be computer simulation results, perhaps in the parametrized form reported by Lambert et al.[47] for linear chains. The results presented here show that this strategy is not possible with LCT at its present state of development.

In terms of its absolute accuracy for the branched system, the LCT theory fares a bit better. When the LCT results are compared directly against the corresponding simulations, the athermal theory is found to be rather good for athermal systems, with some deterioration at the higher chain length. (This will be addressed more fully below.) At $T = 3$, the predictions of LCT2-2 are in *better* agreement with simulation for the branched polymer system than for the linear system. In fact, one can reasonably argue that the LCT2-2 is globally a better theory for the branched system than for the linear system. For the complete set of cases studied here, LCT2-2 certainly produces more generally accurate results than *any* theory that presumes chain architecture to be of no importance whatsoever. However, our study is too limited to conclude that LCT2-2 will always prove superior for branched systems of arbitrary architecture. It is likely that some of the success of LCT2-2 for branched systems at lower temperature arises from a cancellation of errors. In the LCT, a variety of competing effects (temperature, volume fraction, chain length, and architecture) must be taken into account simultaneously via two truncated expansions. It now seems clear that the terms which consider these effects within the LCT interact in a complex way and that the absolute accuracy of the theory must still be addressed on a case-by-case basis.

Table 1. Occupancy Function of Sites Neighboring a Polymer Bead of Specified Valency ($M = 10$, $\phi_p = 0.8$)

T	valence	ν^a	$\nu_{nc}{}^b$
∞	1	0.778	0.734
∞	2	0.807	0.711
∞	3	0.872	0.743
3	1	0.800	0.760
3	2	0.823	0.735
3	3	0.878	0.756

[a] ν is the fraction of all nearest-neighbor sites occupied by a polymer bead. [b] ν_{nc} is the fraction of noncovalent nearest-neighbor sites occupied by a polymer bead.

In an attempt to understand why, or at least how, the solution of branched polymer achieves a higher energy of mixing, we have performed additional simulations for $\phi_p = 0.8$ and $M = 10$ in which we keep track of the number of polymeric nearest neighbors to beads of a given valence (1, 2, or 3). These results are summarized in Table 1, which shows the fraction ν of all nearest-neighbor sites occupied by polymer for beads of various valences. As expected, beads of higher valences have a higher fraction of neighboring polymer beads because there are always two or three covalently bonded beads adjacent to the bead in question. Table 1 also shows the fraction of available *noncovalent* contact sites ν_{nc} occupied by polymer. This quantity is always less than 0.8 for beads of all valences, since the covalent neighbors always serve to increase the local population of polymer beads. The remaining nearby sites must then contain an excess of solvent to produce a local polymer volume fraction near the global value of 0.8. The occupancy fraction ν_{nc} does not change monotonically with valence, and the table shows that the probability of finding another polymer bead at an available noncovalent neighbor site is higher for monovalent and trivalent beads than for divalent beads. This is most likely a consequence of *intra*molecular monovalent–trivalent contacts of the sort indicated by arrows in Figure 1b. Since the increase in the energy of mixing for the branched system requires a net *decrease* in the number of polymer–polymer contacts, this must occur preferentially at the divalent beads.

In Figure 8, we show how the internal energy of mixing for chains of length 10 varies with reciprocal temperature at $\phi_p = 0.6$ and at $\phi_p = 0.8$. From eq 5 and $[\partial(\beta A)/\partial\beta]_{N,V} = E$, one obtains a perturbation series for the internal energy

$$\frac{\Delta E^{MIX}}{N\Delta\epsilon} = e_1 + e_2\left(\frac{\Delta\epsilon}{kT}\right) + e_3\left(\frac{\Delta\epsilon}{kT}\right)^2 + \dots \quad (8)$$

where there is a one-to-one correspondence with the coefficients of eq 5:

$$e_n = na_n \quad (9)$$

The intercepts in the figure are just e_1 for the two systems, while the initial slope is e_2. Any deviation from linearity is evidence of contributions from third- and higher-order terms. Earlier work by Madden et al.[32] and by Dudowicz et al.[33] for chains of mean length 100 suggests that the e_3 and e_4 terms are quite significant at $\phi = 0.6$, and this is again clearly indicated in the figure for both the linear and branched chains. These higher order dependences are believed to be a consequence of conformational changes within chains as polymer–polymer contacts are energetically favored. At lower volume fractions and lower temperatures, the intramolecular contacts that lead to the collapse of isolated chains become increasingly important. The exact e_2 may be obtained from the initial slope of simulation data. The predictions of an *exact* second-order theory is indicated by a solid line, while the results of

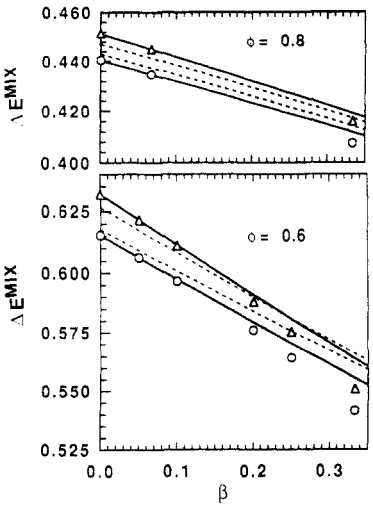

Figure 8. Dependence of the energy of mixing $\Delta E^{MIX}/(N\Delta\epsilon)$ for chains of length 10 on reciprocal temperature, $\beta = \Delta\epsilon/kT$. Circles give the simulation results for linear chains, triangles for branched chains. Solid lines are the results of an exact second-order theory, with coefficients deduced from simulation. Dashed lines are the LCT2-2 predictions. Note that the scale of the figure is highly expanded.

LCT2-2 are shown as dashed lines. The absence of discernible curvature in the LCT2-2 results illustrates that the EMF predictions for e_3 and e_4 are not satisfactory. No lattice theory known to us properly accounts for the curvature in these data at $\phi = 0.6$. Like LCT2-2, any higher order terms that may be present do not include any consideration of the connectivity of the chains and all have higher order temperature dependences comparable to the ineffectual EMF e_3 and e_4.

At the higher volume fraction, both the LCT and the simulations seem to suggest that the energy of mixing is far less dependent on temperature. Only a very slight degree of nonlinearity is present. (The calculations of Madden et al.[32] suggest that it is virtually nonexistent at $\phi = 0.9$.) These conditions favor a low-order perturbation theory, and the predictions of second-order LCT are expected to be rather accurate. The cancellation of errors in the e_1 and e_2 terms improves the LCT2-2 prediction for the branched system at some temperatures. When the monomeric species is interpreted as a vacancy, an n-component lattice theory is also a theory for compressible systems with one fewer component. Under normal melt state conditions, the volume fraction of vacancies that must be invoked to fit experimental data is typically less than 0.15 and an accurate first-order theory for the holes may then be satisfactory. Thus, LCT2-2 may yet be a suitable theory for the equation of state of compressible branched melts. The situation is considerably less clear for systems with a large amount of "free volume", such as supercritical mixtures of polymer and solvent, where the implied volume fraction of voids can be quite high.

We have estimated the exact e_2 at a variety of volume fractions by differences of the energies of mixing at some finite high temperature T^* and the athermal energy of mixing ($T = \infty$):

$$e_2 \cong T^*[\Delta E^{MIX}(T^*) - \Delta E^{MIX}(\infty)] \qquad (10)$$

The temperature T^* must be chosen low enough so that the differences in internal energies of mixing substantially exceed their individual uncertainties but still high enough that the higher order e_n make no measurable contributions. At lower volume fractions, we have found that T^* must be as high as 30 for this situation to be valid. This requires

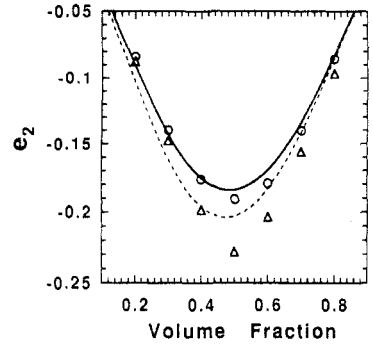

Figure 9. Second-order contribution to the expansion of the internal energy. Circles give the simulation results for linear chains, triangles for branched chains. Solid line is the LCT2-2 result for linear chains. Dashed line is the LCT2-2 result for branched chains.

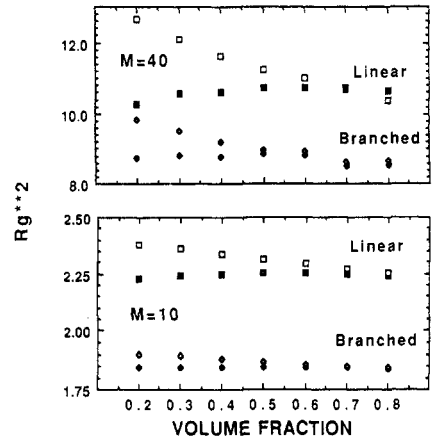

Figure 10. Monte Carlo results for the mean square of radius of gyration for polymer chains of various architectures: open symbols, athermal simulations ($T = \infty$); solid symbols, $T = 3.0$.

careful simulations for $\phi \leq 0.3$ fractions because the energies of mixing are themselves small. We have used $30 \geq T^* \geq 15$ in constructing Figure 9. The second-order term for the branched system seems to somewhat more negative than that of the linear system at all volume fractions considered. The results of LCT2-2 also show this behavior, but the theory underestimates the magnitude of e_2 for the branched system at intermediate volume fractions and overestimates the magnitude at lower volume fractions. The simulation results show an especially large e_2 for the branched system near $\phi = 0.5$. This behavior was confirmed by duplicate calculation of e_2 with several values of T^*.

Figure 10 shows the behavior of the mean square radii of gyration as a function of volume fraction. In the athermal solutions, there is a reduction of radius for both kinds of chains as the volume fraction of polymer is increased. This is expected because the expansive effects of excluded volume on chain dimensions are more completely screened out as the system approaches melt concentrations. The mean square radii of gyration of the branched chains are naturally smaller than those of the linear chains of the same molecular weight. For ideal athermal chains, with no excluded volume, the mean square radii of gyration should scale roughly as the backbone length. For long branched chains with the architecture considered here, the backbone length is 2/3 that of a linear chain of the same molecular weight. However, for both $M = 10$ and $M = 40$, the ratios of the mean square radii of gyration (branched/linear) range from 0.78 to 0.82, indicating that the branched chains are somewhat extended.

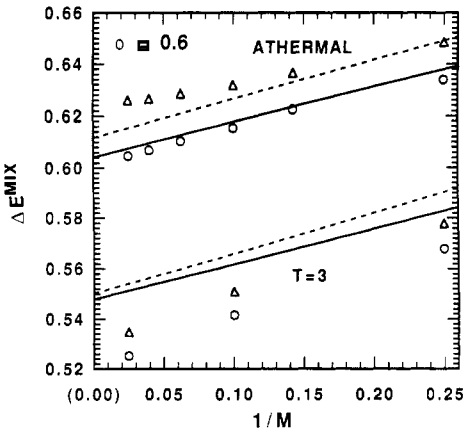

Figure 11. Dependence of the energy of mixing $\Delta E^{MIX}/(N\Delta\epsilon)$ for solvent on reciprocal molecular weight, $1/M$. Circles give the athermal simulation results for linear chains, triangles for branched chains. Solid lines are the LCT2-2 results for linear chains. Dashed lines are the LCT2-2 results for branched chains.

Though the shortness of the chains is an issue, the principal origin of this observation is almost certainly the increased stiffness of the branched chains arising from the finite size of the pendant side groups. That stiffness increases as additional short side chains are added to the backbone. In extreme cases (e.g., four single-bead side chains on every other backbone bead), the chains would be constrained to rigid rod configurations, and the ratio would then diverge with increasing molecular weight. (This is true for the simple-cubic lattice employed in these studies. However, the stiffening effect will depend in a sensitive way on the coordination number of the lattice, becoming less pronounced as the coordination number increases.) As expected, the mean square end-to-end vectors for chains of length 40 also show a ratio (branched/linear) in the neighborhood of 0.8. The ratio of the mean square end-to-end vectors for chains of length 10 is only about 0.69. This is not surprising since the chains are so short. Any similarity with the ideal ratio of 2/3 is almost surely coincidental.

For $T = 3$, the radii of gyration for chains of both linear and branched architectures appear to increase slightly from low to intermediate volume fractions and then level off or fall slightly at higher volume fractions. At higher volume fractions, the explanation for the decrease in radius is again the onset of melt screening (of both the excluded volume and the nearest-neighbor attractions). At lower volume fractions, the chains are contracted because the attractive interactions with noncovalently bonded neighbor beads influence the chain conformations. As expected, the radii of gyration from the thermal and athermal calculations converge at high volume fractions because the effects of the nearest-neighbor forces have little effect on the structure as one approaches melt conditions. The data for $M = 10$ illustrate this point clearly, but the data for $M = 40$ are less consistent at the highest volume fractions. As noted earlier, the poorer quality of the data are probably associated with the shortness of several of the runs and a possible correlation to the initial configurations. Longer runs for $M = 40$ would almost assuredly show the smooth trends observed for the shorter chains. Since the data for the internal energy of mixing (our principal interest in this study) show no such anomalies, we did not pursue this issue further.

Figure 11 shows the molecular weight dependence of the athermal internal energy of mixing for $\phi = 0.6$. The LCT results for the energy of mixing of both branched and linear chains are essentially linear functions of $1/M$, which basically reflects a dilution of end beads by the addition of interior beads. (This quasi-linearity is observed in the LCT2 results at all volume fractions considered here.) While the simulation energies of mixing for linear chains seem to vary as $1/M$ for higher molecular weights, the corresponding results for branched chains show substantial curvature. We have already noted that the radii of gyration for branched chains reveal a somewhat expanded structure. This expansion was attributed to an increase in effective stiffness and hence an increase in the Kuhn length. On that length scale, the branched chains of a given molecular weight are thus effectively shorter than linear chains of the same molecular weight. We suspect that the character of the chain end for the branched polymer is probably not confined just to the immediate region of the terminal beads. When the chains are short, that character may not be completely developed and will evolve as they become longer. Only when the end sequences become fully developed will a simple dilution argument apply. The slope of the energy of mixing with chain length would then depend on the effective molecular weight of the uniquely solvated end sequences. Whether or not this is a complete explanation for the peculiar molecular weight dependence of the branched system, it is clear from Figure 11 that the level of error observed in the LCT2-2 results will not worsen substantially as chain length is further increased.

4. Summary and Conclusions

Computer simulations show that the internal energy of mixing for lattice polymers with monomeric solvent or holes is affected by the presence of short branches on the backbone of the chain. Only the lattice cluster theory of Freed and co-workers predicts any effect of branching on the internal energy. For the particular system studied, the internal energies for athermal mixing are in rather good agreement with simulation for chains of length 10 but are underestimated for athermal chains of length 40. When the temperature is reduced, the agreement with simulation deteriorates somewhat. However, LCT predictions for $T = 3$ are actually in better agreement with simulation for the branched chains than for linear chains. Unfortunately, this means that the effects of branching cannot be reliably predicted within the LCT. These observations emphasize that additional terms in the LCT will be required to achieve satisfactory agreement with the simulations under all conditions of density, temperature, and backbone architecture. Fortunately, second-order theories are probably adequate to include the effects of compressibility on the properties of simple polymer melts.

Deficiencies in the e_1 and e_2 terms for branched systems suggest that higher order terms in the $1/z$ expansions will be necessary to achieve quantitative accuracy at high temperature. One can expect that this is also an issue in the purely entropic contributions to the free energy. The convergence of the LCT expansions depends in large measure on the magnitude of the coordination number z. On an FCC or BCC lattice, the theory might be considerably improved, though the effects of branching would be expected to be somewhat reduced. Unfortunately, detailed expressions for such cases are not yet available within the LCT. Since simple models for polymers in the continuum pack with coordination numbers higher than 6, we might guess that, for such systems, branching will have less effect than that observed in this study. However, additional complexity is possible in the continuum, since covalent bonds are generally much shorter than cohesive

contacts and different elements have different characteristic sizes. In an atomically faithful rendition of a real polymer, the distribution of material in the neighborhood of a divalent atom may be quite different than that about a trivalent or monovalent atom or about a divalent atom of a different element.

Additional studies are now underway to calculate the lattice pressure (excess chemical potential of solvent) for linear and branched chains of the sort examined here. These studies will provide a direct assessment of the predictions of the theory for the athermal ("entropic") contribution to the free energy of mixing. Studies are also being made on lattices of higher coordination number.

References and Notes

(1) Flory, P. J. *J. Chem. Phys.* **1941**, *9*, 660.
(2) Flory, P. J. *J. Chem. Phys.* **1942**, *10*, 51.
(3) Flory, P. J. *Principles of Polymer Chemistry*; Cornell University Press: Ithaca, NY, 1953; Chapter XII.
(4) Huggins, M. L. *J. Chem. Phys.* **1941**, *9*, 440.
(5) Huggins, M. L. *J. Phys. Chem.* **1942**, *46*, 151; *Ann. N.Y. Acad. Sci.* **1942**, *41*, 1.
(6) Miller, A. R. *Proc. Cambridge Philos. Soc.* **1942**, *38*, 109.
(7) Miller, A. R. *Proc. Cambridge Philos. Soc.* **1943**, *39*, 54.
(8) Guggenheim, E. A. *Proc. R. Soc. London Ser. A* **1944**, *183*, 203.
(9) Guggenheim, E. A. *Proc. R. Soc. London Ser. A* **1944**, *183*, 213.
(10) Guggenheim, E. A. *Mixtures*; Oxford University Press: Oxford, 1952.
(11) Sanchez, I. C.; Lacombe, R. H. *Macromolecules* **1978**, *11*, 1145.
(12) Panayiotou, C.; Vera, J. H. *Polym. J.* **1982**, *14*, 681.
(13) Kumar, S. K., Reid, R. C.; Suter, U. W. *Prepr. Pap.—Am. Chem. Soc., Div. Fuel Chem.* **1985**, *30*, 66; *Ind. Eng. Chem.* **1987**, *26*, 2532. Kumar, S. K.; Chabria, S. K.; Reid, R. C.; Suter, U. W. *Macromolecules* **1987**, *20*, 2550.
(14) Prigogine, I. *The Molecular Theory of Solutions*; North-Holland: Amsterdam, 1957.
(15) Flory, P. J.; Orwoll, R. A.; Vrij, A. *J. Am. Chem. Soc.* **1964**, *86*, 3507.
(16) Dee, G. T.; Walsh, D. J. *Macromolecules* **1988**, *21*, 815.
(17) Wertheim, M. S. *J. Chem. Phys.* **1987**, *87*, 7323.
(18) Schweitzer, K. S.; Curro, J. G. *Phys. Rev. Lett.* **1987**, *58*, 246; *J. Chem. Phys.* **1988**, *89*, 3342; **1989**, *91*, 5059; *Macromolecules* **1988**, *21*, 3070; *Chem. Phys.* **1990**, *149*, 105; *J. Chem. Phys.* **1991**, *94*, 3986. Curro, J. G.; Schweitzer, K. S. *J. Chem. Phys.* **1987**, *87*, 1842; *Macromolecules* **1990**, *23*, 1402 and references therein.
(19) Chiew, Y. C. *J. Chem. Phys.* **1990**, *93*, 5067; *Mol. Phys.* **1991**, *73*, 359.
(20) Freed, K. F. *J. Phys. A* **1985**, *18*, 871.
(21) Bawendi, M. G.; Freed, K. F. *J. Chem. Phys.* **1986**, *85*, 3007.
(22) Bawendi, M. G.; Freed, K. F. *J. Chem. Phys.* **1988**, *88*, 2741.
(23) Bawendi, M. G.; Freed, K. F.; Mohanty, U. *J. Chem. Phys.* **1987**, *87*, 5534.
(24) Pesci, A. I.; Freed, K. F. *J. Chem. Phys.* **1989**, *90*, 2003, 2017.
(25) Nemirovsky, A. M.; Bawendi, M. G.; Freed, K. F. *J. Chem. Phys.* **1987**, *87*, 7272. Bawendi, M. G.; Freed, K. F.; Mohanty, U. *J. Chem. Phys.* **1986**, *84*, 7036. Pesci, A. I.; Freed, K. F. *J. Chem. Phys.* **1987**, *87*, 7342.
(26) Freed, K. F.; Bawendi, M. G. *J. Phys. Chem.* **1989**, *93*, 2194.
(27) Dickman, R.; Hall, C. K. *J. Chem. Phys.* **1986**, *85*, 3023.
(28) Dickman, R. *Chem. Phys.* **1989**, *91*, 454; **1990**, *93*, 774.
(29) Dickman, R.; Hall, C. K. *J. Chem. Phys.* **1988**, *89*, 3168.
(30) Hertando, A.; Dickman, R. *J. Chem. Phys.* **1988**, *89*, 7577.
(31) Dickman, R. *Chem. Phys.* **1987**, *87*, 2246.
(32) Madden, W. G.; Pesci, A. I.; Freed, K. F. *Macromolecules* **1990**, *23*, 1181.
(33) Dudowicz, J.; Freed, K. F.; Madden, W. G. *Macromolecules* **1990**, *23*, 4803.
(34) Sariban, A.; Binder, K. *J. Chem. Phys.* **1987**, *86*, 5859.
(35) Sariban, A.; Binder, K.; Heerman, D. W. *Colloid Polym. Sci.* **1987**, *265*, 424. Sariban, A.; Binder, K. *Colloid Polym. Sci.* **1988**, *266*, 389; **1989**, *267*, 469.
(36) Sariban, A.; Binder, K. *Macromolecules* **1988**, *21*, 711.
(37) Sariban, A.; Binder, K.; Heermann, D. W. *Phys. Rev. B* **1987**, *B35*, 6873.
(38) Lipson, J. E. G.; Guillet, J. E.; Whittington, S. G. *Macromolecules* **1985**, *18*, 573.
(39) Lipson, J. E. G. *Macromolecules* **1991**, *24*, 1334.
(40) Lipson, J. E. G. *J. Chem. Phys.* **1992**, *96*, 1418.
(41) Lipson, J. E. G.; Andrews, S. S. *J. Chem. Phys.* **1992**, *96*, 1426.
(42) Verdier, P.; Stockmayer, W. H. *J. Chem. Phys.* **1962**, *36*, 227.
(43) Mansfield, M. L. *J. Chem. Phys.* **1982**, *77*, 1554.
(44) Olaj, O. F.; Lantschbauer, W.; Pelinka, K. H. *Chem. Kunstst. Aktuelle* **1978**, *32*, 199. Olaj, O. F.; Lantschbauer, W. *Makromol. Chem., Rapid Commun.* **1982**, *3*, 847.
(45) Madden, W. G. *J. Chem. Phys.* **1987**, *87*, 1405; **1988**, *88*, 3934.
(46) Mathur, S. C.; Rodrigues, K.; Mattice, W. L. *Macromolecules* **1989**, *22*, 2781.
(47) Lambert, S. M.; Soane, D. S.; Prausnitz, J. M., preprint of a talk given at the Sixth International Conference on Fluid Properties and Phase Equilibria, Cortina, Italy, 1992.